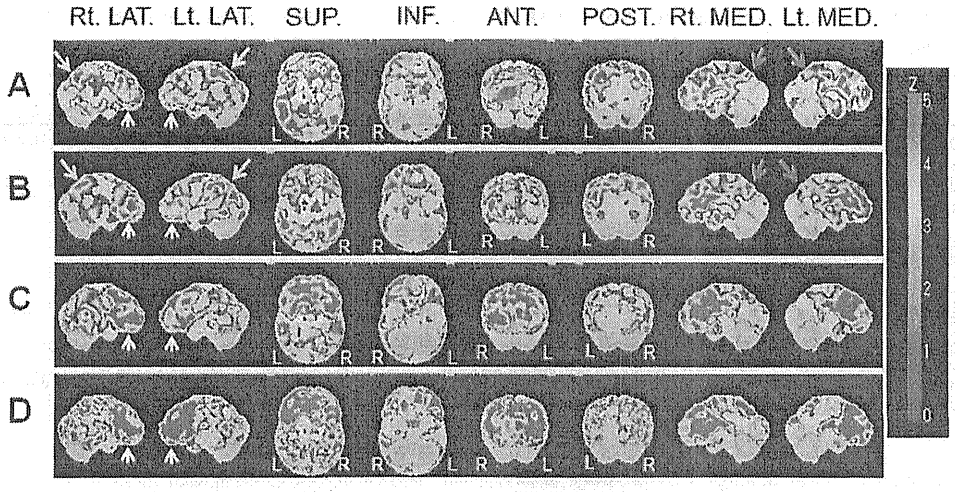

Figure 3. Cerebral blood flow SPECT images. A, B, C, and D show Z-score maps of SPECT images taken when the patient was 34 and 35 years old, after the onset of convulsive seizures when the patient was 36 years old, and one month after the convulsive seizures, respectively. A positive Z score represents a decrease in the regional CBF in the patient relative to the control mean. The red arrows indicate diminished blood flow to the posterior parietal area, including the precuneus. The yellow and white arrows indicate diminished blood flow to the parietal lobe and frontal lobe, respectively. Diminished blood flow to the precuneus, frontal lobe, and parietal lobe was noted even before the onset of convulsive seizures (A, B). After the seizures, however, blood flow to the frontal lobe was markedly diminished (C) and became progressively worse (D). LAT.: lateral, SUP.: superior, INF.: inferior, ANT.: anterior, POST.: posterior, MED.: medial

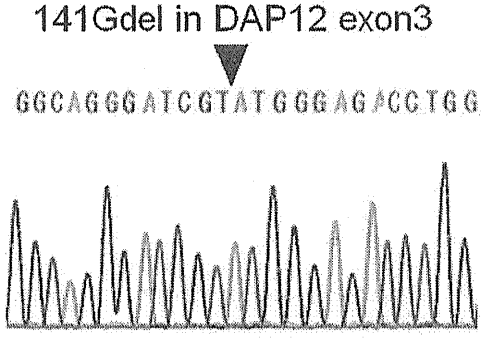

Figure 4. Sequencing analysis of the DAP12 gene. Exons and exon-intron boundaries of the DAP12 gene were amplified from genomic DNA by a polymerase chain reaction (PCR). PCR products were processed for direct sequencing analysis. The figure represents a single-base deletion of 141G (141delG) in exon 3. This genetic mutation was found to be a homozygous point mutation.

onstrated DAP12 gene mutation.

Discussion

The present case is the fifth case of NHD reported in the world with a homozygous mutation (single-base deletion) of 141delG in exon 3 of the DAP12 gene. All reported cases of DAP12 gene mutation (141delG) (3, 6), including the present case, have been Japanese, which suggests that this type of genetic mutation may be specific to the Japanese population.

The clinical characteristics of typical cases of defects in the DAP12 and TREM12 genes reported in the previous studies and the characteristics of the present case are summarized in Table 2 (4, 7). Compared to the previous cases, the present case exhibited an earlier onset of frontal lobe and bone symptoms and a shorter period before the patient became bedridden.

The DAP12 gene mutation (141delG) of the present case involved a frameshift of the open reading frame and the coding of the truncated DAP12 protein with no intracellular tyrosine-based activation motif (ITAM) (8), which can potentially lead to the dysfunction of TREM2/DAP12 signaling cascades. According to the previous reports, TREM2/DAP12 signaling cascades play an important role in immune regulation, including the stimulation of mononuclear phagocytes in the central nervous system (5, 10). Genetic defects lead to the dysfunction of TREM2/DAP12 signaling cascades expressed in the cell membrane of microglia. Under this circumstance, apoptotic nerve cells can no longer be removed by phagocytosis; as a result, the inflammation persists and becomes protracted. These processes are believed to make up the pathological mechanism that underlies the central nervous system damage observed in NHD.

In the present case, rapid progression of brain damage was observed after the onset of prolonged convulsive sei-

Table 2. Comparison of Clinical Symptoms between the Cases Reported Previously and the Case Examined in the Present Study

	Mutation	N (patients)	Age at onset of frontal lobe syndrome (years)	Age at onset of bone pain and fracture (years)	Epileptic seizure	Age at onset of abasia (years)
Paloneva (4) (2001)	DAP12 gene; Del 5.3kb	8	25-40 (mean, 33)	18-33 (mean, 27)	7/8 (87.5 %)	34-47 (mean, 42.5)
Klünemann (7) (2005)	TREM2 gene; 97C > T, 267delG, 313delG, 377T > G	6	22-39 (mean, 33)	21-40 (mean, 31)	ND	ND
Present case	DAP12 gene; 141delG	1	26	18	+	36

ND: Not described

A comparison was made between the clinical characteristics of typical cases of defects in the DAP12 and TREM12 genes reported in previous studies[4,7] and the characteristics of the case reported in the present study

zures. The promotion of brain damage was possibly caused by a failure to phagocytize and delete the apoptotic neurons resulting from the severe epileptic seizures. The control of epileptic seizures is believed to be effective in preventing the progression of brain damage.

The present SPECT findings showed regional cerebral blood flow (rCBF) abnormalities to the cerebral cortex, including the frontal and parietal lobes. These findings were consistent with previously reported results of SPECT and positron emission tomography (PET) images in NHD (7, 12, 13). Unlike the previous reports in which SPECT images were analyzed qualitatively, the present study was designed to identify a statistical image analysis using 3D stereotactic surface projections (3D-SSP). In this way, we were able to examine diminished blood flow to the parietal lobe in a more detailed manner, and we successfully identified diminished blood flow to the posterior parietal area, including the precuneus. The results of the overall psychological tests disclosed the neuropsychological profiles, that is, intact overall cognitive function with memory decline as primary disturbances that resembled MCI (14). SPECT and PET studies of MCI have demonstrated diminished blood flow and metabolism in the posterior cingulate gyrus and precuneus, which are known to have dense fiber connections with medial temporal lesions, such as the hippocampus (15-17). These findings are an important determinant in the diagnosis of MCI, which is believed to be a precursor to Alzheimer's disease. In the present case, the diminished blood flow to the precuneus was also suspected to be the distant effect of hippocampal disorder. On the other hand, the close relationship between the precuneus and spatially guided behaviour is becoming clear (18). The precuneus disorder might be a cause of the memory impairment that is similar to MCI and the characteristic visuo-spatial memory impairment of NHD (19).

NHD is an intractable disease accompanied by symptoms of early-onset dementia. There has been a report of a case of a TREM2 gene mutation in a patient who manifested symptoms of dementia without exhibiting bone lesions (9). Similarly, there have been two reported cases of heterozygous carriers of the mutated allele of TREM2 gene mutation who had profound visuo-spatial memory impairment without exhibiting bone lesions and whose SPECT study revealed the diminished blood flow to the basal ganglia (19). Although NHD is a rare disease, we believe it has important implications in the identification of early-onset dementia accompanied mainly by frontal lobe symptoms.

The authors state that they have no Conflict of Interest (COI).

References

1. Hakola HPA. Neuropsychiatric and genetic aspects of a new hereditary disease characterized by progressive dementia and lipomembranous polycystic osteodysplasia. Acta Psychiatr Scand 232 (suppl): 1-173, 1972.
2. Nasu T, Tsukahara Y, Terayama K. A lipid metabolic disease-"membranous lipodystrophy"-an autopsy case demonstrating numerous peculiar membrane-structures composed of compound lipid in bone and bone marrow and various adipose tissues. Acta Pathol Jpn 23: 539-558, 1973.
3. Paloneva J, Kestilä M, Wu J, et al. Loss-of-function mutations in TYROBP (DAP12) result in a presenile dementia with bone cysts. Nat Genet 25: 357-361, 2000.
4. Paloneva J, Autti T, Raininko R, et al. CNS manifestations of Nasu-Hakola disease: a frontal dementia with bone cysts. Neurology 56: 1552-1558, 2001.
5. Bianchin MM, Capella HM, Chaves DL, et al. Nasu-Hakola disease (polycystic lipomembranous osteodysplasia with sclerosing leukoencephalopathy--PLOSL): a dementia associated with bone cystic lesions. From clinical to genetic and molecular aspects. Cell Mol Neurobiol 24: 1-24, 2004.
6. Kondo T, Takahashi K, Kohara N, et al. Heterogeneity of presenile dementia with bone cysts (Nasu-Hakola disease): three genetic forms. Neurology 59: 1105-1107, 2002.
7. Klünemann HH, Ridha BH, Magy L, et al. The genetic causes of basal ganglia calcification, dementia, and bone cysts: DAP12 and TREM2. J. Neurology 64: 1502-1507, 2005.
8. Kuroda R, Satoh J, Yamamura T, et al. A novel compound heterozygous mutation in the DAP12 gene in a patient with Nasu-Hakola disease. J Neurol Sci 252: 88-91, 2007.
9. Chouery E, Delague V, Bergougnoux A, Koussa S, Serre JL, Mégarbané A. Mutations in TREM2 lead to pure early-onset dementia without bone cysts. Hum Mutat 29: E194-E204, 2008.
10. Neumann H, Takahashi K. Essential role of the microglial triggering receptor expressed on myeloid cells-2 (TREM2) for central nervous tissue immune homeostasis. J Neuroimmunol 184: 92-99,

2007.

11. Minoshima S, Frey KA, Koeppe RA, Foster NL, Kuhl DE. A diagnostic approach in Alzheimer's disease using three-dimensional stereotactic surface projections of fluorine-18-FDG PET. J Nucl Med **36**: 1238-1248, 1995.
12. Ueki Y, Kohara N, Oga T, et al. Membranous lipodystrophy presenting with palilalia: a PET study of cerebral glucose metabolism. Acta Neurol Scand **102**: 60-64, 2000.
13. Takeshita T, Kaminaga T, Tatsumi T, Hatanaka Y, Furui S. Regional cerebral blood flow in a patient with Nasu-Hakola disease. Ann Nucl Med **19**: 309-312, 2005.
14. Petersen RC. Mild cognitive impairment as a diagnostic entity. J Intern Med **256**: 183-194, 2004.
15. Minoshima S, Giordani B, Berent S, Frey KA, Foster NL, Kuhl DE. Metabolic reduction in the posterior cingulate cortex in very early Alzheimer's disease. Ann Neurol **42**: 85-94, 1997.
16. Kogure D, Matsuda H, Ohnishi T, et al. Longitudinal evaluation of early Alzheimer's disease using brain perfusion SPECT. J Nucl Med **41**: 1155-1162, 2000.
17. Chételat G, Desgranges B, de la Sayette V, et al. Dissociating atrophy and hypometabolism impact on episodic memory in mild cognitive impairment. Brain **126**: 1955-1967, 2003.
18. Cavanna A, Trimble MR. The precuneus: a review of its functional anatomy and behavioural correlates. Brain **129**: 564-583, 2006.
19. Montalbetti L, Ratti MT, Greco B, Aprile C, Moglia A, Soragna D. Neuropsychological tests and functional nuclear neuroimaging provide evidence of subclinical impairment in Nasu-Hakola disease heterozygotes. Funct Neurol **20**: 71-75, 2005.

nan_1206

Neuropathology and Applied Neurobiology (2011) doi: 10.1111/j.1365-2990.2011.01206.x

Immunohistochemical characterization of γ-secretase activating protein expression in Alzheimer's disease brains

J. Satoh*, H. Tabunoki*, T. Ishida†, Y. Saito‡ and K. Arima§

**Department of Bioinformatics and Molecular Neuropathology, Meiji Pharmaceutical University, Tokyo, †Department of Pathology and Laboratory Medicine, Kohnodai Hospital, NCGM, Chiba, ‡Department of Laboratory Medicine, National Center Hospital, NCNP, Tokyo, and §Department of Psychiatry, National Center Hospital, NCNP, Tokyo, Japan*

J. Satoh, H. Tabunoki, T. Ishida, Y. Saito and K. Arima (2011) *Neuropathology and Applied Neurobiology*
Immunohistochemical characterization of γ-secretase activating protein expression in Alzheimer's disease brains

1 **Aims:** A recent study showed that γ-secretase activating protein (GSAP), derived from a C-terminal fragment of pigeon homolog (PION), increases amyloid-β (Aβ) production by interacting with presenilin-1 (PS1) and the β-secretase-cleaved C-terminal fragment of amyloid pre-
2 cursor protein (APP-CTF). In the study, knockdown of GSAP reduces production of Aβ and plaque formation in the brain of APPswe and PS1ΔE9 double transgenic mice without affecting the Notch-dependent pathway. Therefore, GSAP is an ideal target for designing γ-secretase modulators with least side effects in Alzheimer's disease (AD). However, at present, the precise distribution of GSAP in AD brains remains to be characterized. **Methods:** By immunohistochemistry, we studied GSAP expression in the frontal cortex and the hippocampus of 11 aged AD and 17 age-matched control cases. **Results:** GSAP immunoreactivity exhibited distinct morphological features, such as fine granular cytoplasmic deposits, dense nodular and patchy deposits, beads and string-like deposits, and diffuse dot-like deposits. In both AD and control brains, a fairly small subset of cerebral cortical and hippocampal neurones expressed fine granular cytoplasmic deposits, while diffuse dot-like deposits were more frequently found in the neuropil and neuronal processes, particularly enriched in the hippocampal CA2 and CA3 regions. Among GSAP-immunoreactive deposits, dense nodular and patchy deposits, located in the neuropil and closely associated with PS1 expression and Aβ deposition, indicated the most distinguishing features of AD pathology. **Conclusions:** Aberrant regulation of GSAP expression plays a key role in acceleration of γ-cleavage of APP-CTF and accumulation of Aβ in AD brains.

Keywords: Alzheimer's disease, amyloid-β, GSAP, immunohistochemistry, PION

Introduction

Alzheimer's disease (AD) is the most common cause of dementia worldwide, affecting the elderly population, characterized by the hallmark pathology of widespread amyloid-β (Aβ) deposition and neurofibrillary tangle (NFT) formation in the brain [1]. The major amyloidogenic peptides Aβ40/Aβ42 are generated by the consecutive cleavage of the amyloid precursor protein (APP) by β-secretase and γ-secretase. The latter forms a complex composed of presenilin-1 (PS1), anterior pharynx defective 1 homolog (APH1), presenilin enhancer 2 homolog (PEN2) and nicastrin. The presenilin complex regulates intramembrane proteolysis not only of

Correspondence: Jun-ichi Satoh, Department of Bioinformatics and Molecular Neuropathology, Meiji Pharmaceutical University, 2-522-1 Noshio, Kiyose, Tokyo 204-8588, Japan. Tel: +81 42 495 8678; Fax: +81 42 495 8678; E-mail: satoj@my-pharm.ac.jp

The authors declare that there is no conflict of interest.

the β-secretase-cleaved C-terminal fragment of APP (APP-CTF) but also of Notch and cadherins, both of which play a pivotal role in transducing biologically essential signals [2]. Development of γ-secretase inhibitors and modulators that reduce Aβ production but do not affect the cleavage of other γ-secretase substrates is the most desirable approach for AD therapy to minimize toxic side effects of these drugs [3].

A previous study showed that an anticancer drug imatinib, named Gleevec, acts as a γ-secretase modulator that reduces production of Aβ38, Aβ40 and Aβ42 by inhibiting γ-cleavage of APP-CTF without affecting Notch processing [4]. Recently, the same group identified a γ-secretase activating protein (GSAP) that facilitates Aβ production by interacting with PS1-CTF and the juxtamembrane region of APP-CTF [5]. They found that GSAP is derived from a C-terminal fragment spanning amino acid residues 733-854 of pigeon homolog (PION), a protein of unknown biological function expressed in various tissues, including the brain. When expressed in cultured cells, the full-length human PION protein is rapidly cleaved, processed into GSAP via an unknown mechanism, and is accumulated in a trans-Golgi network. GSAP modulates γ-cleavage of APP but not of Notch. However, it differentially regulates γ-cleavage and ε-cleavage of APP-CTF. GSAP elevates the levels of Aβ derived from γ-cleavage, whereas it reduces the amount of the APP intracellular domain produced by ε-cleavage. Most importantly, knockdown of GSAP reduces production of Aβ and plaque formation in the brain of APPswe and PS1ΔE9 double transgenic mice without affecting the Notch-dependent pathway [5]. Imatinib actually achieves its Aβ-lowering effect by interfering with GSAP interaction with APP-CTF [5]. Thus, GSAP would represent an ideal target for designing γ-secretase modulators with least side effects for AD therapy [6].

However, at present, the precise distribution of GSAP in AD brains remains unknown. In the present study, we have attempted to characterize GSAP expression in AD brains by immunohistochemistry.

Materials and methods

Human brain tissues

Ten micron-thick serial sections of the hippocampus and the frontal cortex were prepared from autopsied brains of 11 AD patients, composed of five men and six women with the mean age of 71 ± 9 years, and 17 non-AD patients, composed of 10 men and seven women with the mean age of 67 ± 8 years. The non-AD group includes four normal subjects died of non-neurological causes, four patients with myotonic dystrophy, three with Parkinson's disease, two with multiple system atrophy and four with amyotrophic lateral sclerosis. All AD cases were satisfied with the Consortium to Establish a Registry for Alzheimer's Disease criteria for diagnosis of definite AD [7]. Detailed characteristics of the brains employed are shown in Table S1, and were in part described previously [8–10]. All AD brains were categorized into the stage C of amyloid deposition and the stage VI of neurofibrillary degeneration, following the Braak staging system [11,12]. Autopsies on all subjects were performed at the National Center Hospital, National Center of Neurology and Psychiatry, Japan or Kohnodai Hospital, National Center for Global Health and Medicine, Japan. The pathological diagnosis was validated by comprehensive examination of autopsied brains by three established neuropathologists (K. A., Y. S., T. I.). Written informed consent was obtained from all the cases. The Ethics Committee of the corresponding institutions approved the present study.

Immunohistochemistry

The brain tissues were fixed with 4% paraformaldehyde and embedded in paraffin. After deparaffinization, tissue sections were heat-treated in 10 mM citrate sodium buffer, pH 6.0 by autoclaving them at 125°C for 30 s in a temperature-controlled pressure chamber (Dako, Tokyo, Japan). For Aβ immunolabelling, they were pretreated with formic acid for 5 min at room temperature (RT). The tissue sections were exposed at RT for 15 min to 3% hydrogen peroxide-containing methanol to block the endogenous peroxidase activity. They were then incubated with phosphate-buffered saline (PBS) containing 10% normal goat serum at RT for 15 min to block non-specific staining. Subsequently, they were incubated in a moist chamber at 4°C overnight with a rabbit anti-GSAP antibody raised against the peptide spanning amino acid residues 769-840 of the human PION protein, composed of HPMSSNI ISRNHVTRLLQNYKKQPRNSMINKSSFSVEFLPLNYFIEIL TDIESSNQALYPFEGHDNVDAEFV (1:100, HPA020058; Sigma, St. Louis, MO, USA) or a rabbit anti-PION non-GSAP fragment antibody raised against the peptide spanning amino acid residues 471-558 of the human PION protein, composed of SSYWSVYSETSNMDKLLPHSSVLT

WNTEIPGITLVTEDIALPLMKVLSFKGYWEKLNSNLEYVK YAKPHFHYNNSVVRREWHNLISEE (1:100, HPA023994; Sigma). After washing with PBS, the tissue sections were labelled at RT for 30 min with peroxidase-conjugated secondary antibodies (Nichirei, Tokyo, Japan), followed by incubation with diaminobenzidine tetrahydrochloride (DAB) substrate and a DAB-enhancing solution (Vector, Burlingame, CA, USA). They were processed for a counter-stain with haematoxylin. For negative controls, the primary antibody was preabsorbed with recombinant human GSAP protein tagged with Xpress produced by an *E. coli* expression system.

For double-labelling immunohistochemistry, tissue sections were initially stained with mouse anti-PS1 monoclonal antibody (1:100, sc-80297; Santa Cruz Biotechnology, Santa Cruz, CA, USA), mouse anti-Aβ11-28 monoclonal antibody (1:50, 12B2; Immunobiological Laboratory, Gunma, Japan) or mouse anti-PHF-tau monoclonal antibody (1:100, AT8; Thermo Scientific, Rockford, IL, USA), then followed by incubation with alkaline phosphatase-conjugated secondary antibody (Nichirei), and colourized with New Fuchsin substrate (Nichirei). After inactivation of the antibody by autoclaving the sections, they were relabelled with anti-GSAP antibody HPA020058, followed by incubation with peroxidase-conjugated secondary antibody, and colourized with DAB substrate.

Quantification of GSAP-immunoreactive particles

To quantify the number of GSAP-immunoreactive dot-like deposits, the images of three fields intervening between the hippocampal CA2 and CA3 regions at a ×200 magnification under microscope were captured, and processed for quantification of the particle signals with ImageJ software (National Institute of Health, Bethesda, MD, USA). The statistical difference in the average of counts/field between AD and non-AD groups was evaluated by Student's *t*-test.

Results

GSAP immunoreactivity exhibited four distinct morphological features

By immunohistochemistry using the antibody HPA020058, we identified GSAP immunoreactivity in both AD and non-AD brains. The specificity of the antibody was validated by Western blot of the corresponding recombinant protein fragment expressed in HEK293 cells and *E. coli* (Figure S1**a,b,d** and Figure S2**a**). Overall, the distribution of GSAP did not show apparent similarities to the pattern of expression of GFAP, Aβ or tau (Figure 1). In AD and control brains, GSAP-immunoreactive deposits were distributed chiefly in the neuropil and neuronal processes, and occasionally in neuronal cell bodies, vascular walls and perivascular cells. We categorized the morphology of GSAP-immunoreactive deposits into the following four patterns: (i) fine granular deposits located in the cytoplasm of a fairly small subset of cerebral cortical and hippocampal neurones in AD and control brains (Figure 2**a** and Figure 3**d**); (ii) dense nodular and patchy deposits, often being extracellular and forming clusters and clumps, located in the neuropil most frequently identified in AD brains but barely detectable in control brains (Figure 2**b–e**); (iii) beads and string-like deposits located in neuronal processes found in the cortex and the white matter of both AD and control brains (Figure 3**a,b**); and (iv) diffuse dot-like deposits located in the neuropil and neuronal processes, most frequently found in the hippocampal CA2 and CA3 regions of both AD and controls (Figure 3**c**). Thus, we found that dense nodular and patchy deposits located in the neuropil represent the most distinguishing characteristics of AD pathology, because this pattern was hardly found in control brains. The negative controls without inclusion of the primary antibody generated no discernible signals, and the antibody preabsorbed by recombinant GSAP protein produced greatly diminished signals (Figure S2, **c** *vs.* **b**). In contrast to detection of GSAP by immunohistochemistry, we could not detect GSAP expression by Western blot of SDS-soluble protein extract isolated from the frontal cortex of AD and non-AD cases (Figure S1**e**), suggesting the possibility that the amounts of GSAP protein in the frontal cortex are below the detection level for Western blot by the antibody HPA020058, or alternatively that GSAP is sequestered in detergent-insoluble fractions *in vivo*.

The number of GSAP-immunoreactive dot-like deposits varied greatly among the cases

Because GSAP-immunoreactive dot-like deposits were commonly observed in both AD and control brains, we considered the possible scenario that dot-like deposits represent a predecessor of dense nodular and patchy deposits.

Colour

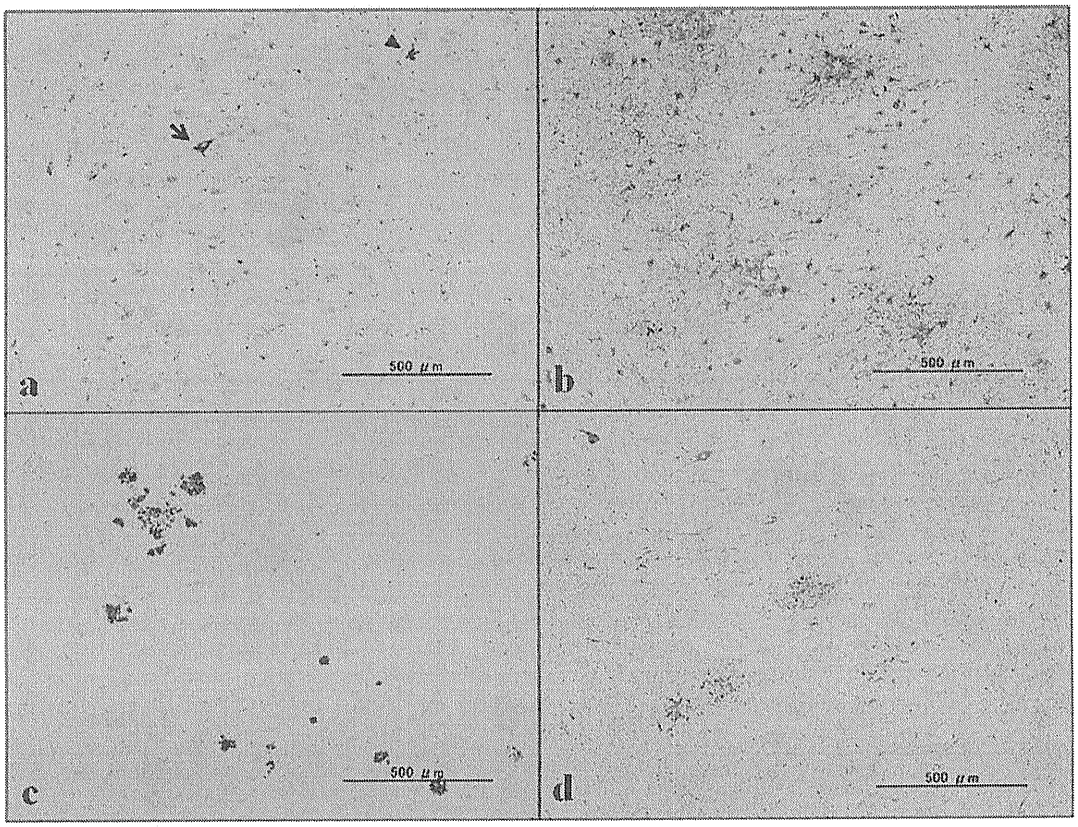

10 **Figure 1.** The expression of γ-secretase activating protein (GSAP), GFAP, amyloid-β (Aβ) and tau in Alzheimer's disease (AD) brains. The panels (**a–d**) represent low magnification photographs of (**a**) GSAP (HPA020058), (**b**) GFAP, (**c**) Aβ and (**d**) tau (AT8) in serial tissue sections of the hippocampal CA3 region of AD. High magnification photographs corresponding to the region indicated by an arrow and an arrowhead in panel (**a**) are shown in Figure 2, panels **a** and **b**, respectively.

Therefore, we quantitatively evaluated the amount of dot-like particles in the hippocampal CA2 and CA3 regions by imaging them on ImageJ software. Contrary to our expectation, we found that the number of particles per field varied greatly among individual cases (Figure 4**a**). Although all AD cases examined in the present study are categorized into the most advanced stages of AD pathology, the number of GSAP-immunoreactive particles was surprisingly small in several AD cases, such as AD5, AD8, AD9 and AD11 (Figure 4**a**).

When the counts of dot-like deposits were compared between AD cases, all of which were categorized into the Braak NFT stage of VI ($n = 11$, the mean age of 71 ± 9 years) and non-AD cases categorized into the stages III/IV compatible with NFT pathology of the early AD ($n = 5$, the mean age of 64 ± 10 years), the difference did not become statistically significant ($P = 0.462$) (Figure 4**b**). However, when they were compared between AD cases and non-AD cases categorized into the stages II/III compatible with NFT pathology of normal ageing and the earliest AD ($n = 9$, the mean age of 74 ± 11 years), the difference became statistically significant ($P = 0.043$) (Figure 4**c**). When the counts of dot-like deposits were compared between the cases with almost no Aβ deposits classified as the stage Zero of amyloid deposition ($n = 8$, the mean age of 66 ± 7 years) and those with extensive Aβ deposits classified as the stage C of amyloid deposition ($n = 13$, the mean age of 71 ± 8 years), the difference did not become statistically significant ($P = 0.926$) (Figure 4**d**). These results suggest that there exists a trend

Colour

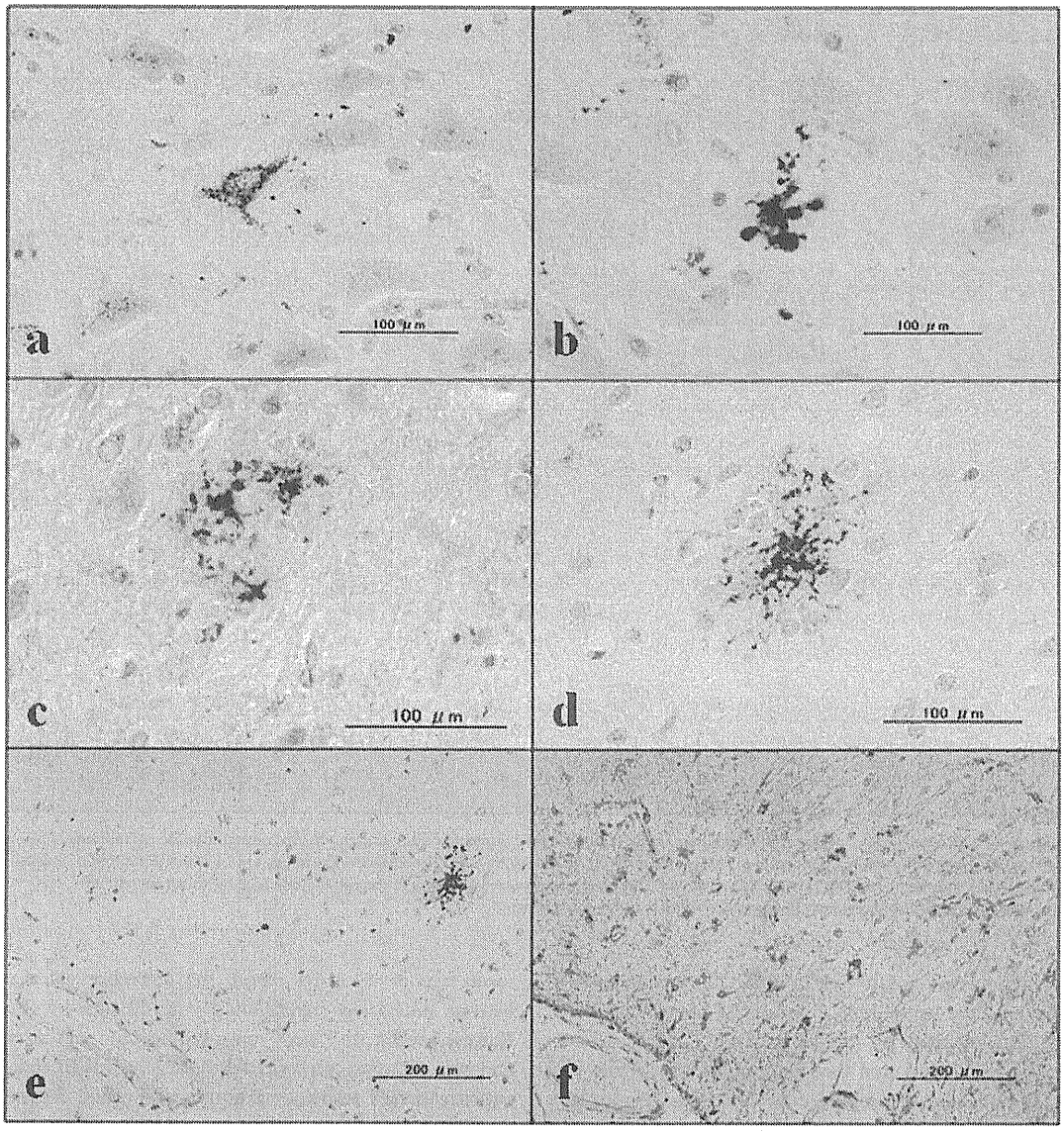

Figure 2. γ-Secretase activating protein (GSAP) expression in Alzheimer's disease (AD) brains. The panels (**a–f**) represent GSAP immunoreactivity of (**a**) fine granular deposits in the neuronal cytoplasm in the hippocampal CA3 region of AD, (**b**) a clump of dense nodular deposits in the neuropil in the hippocampal CA3 region of AD, (**c**) a cluster of dense patchy deposits in the neuropil in the frontal cortex of AD, (**d**) a clump of dense patchy deposits in the neuropil in the frontal cortex of AD, and low magnification photographs of (**e**) the region corresponding to (**d**), and (**f**) GFAP of the serial tissue section corresponding to (**e**).

11

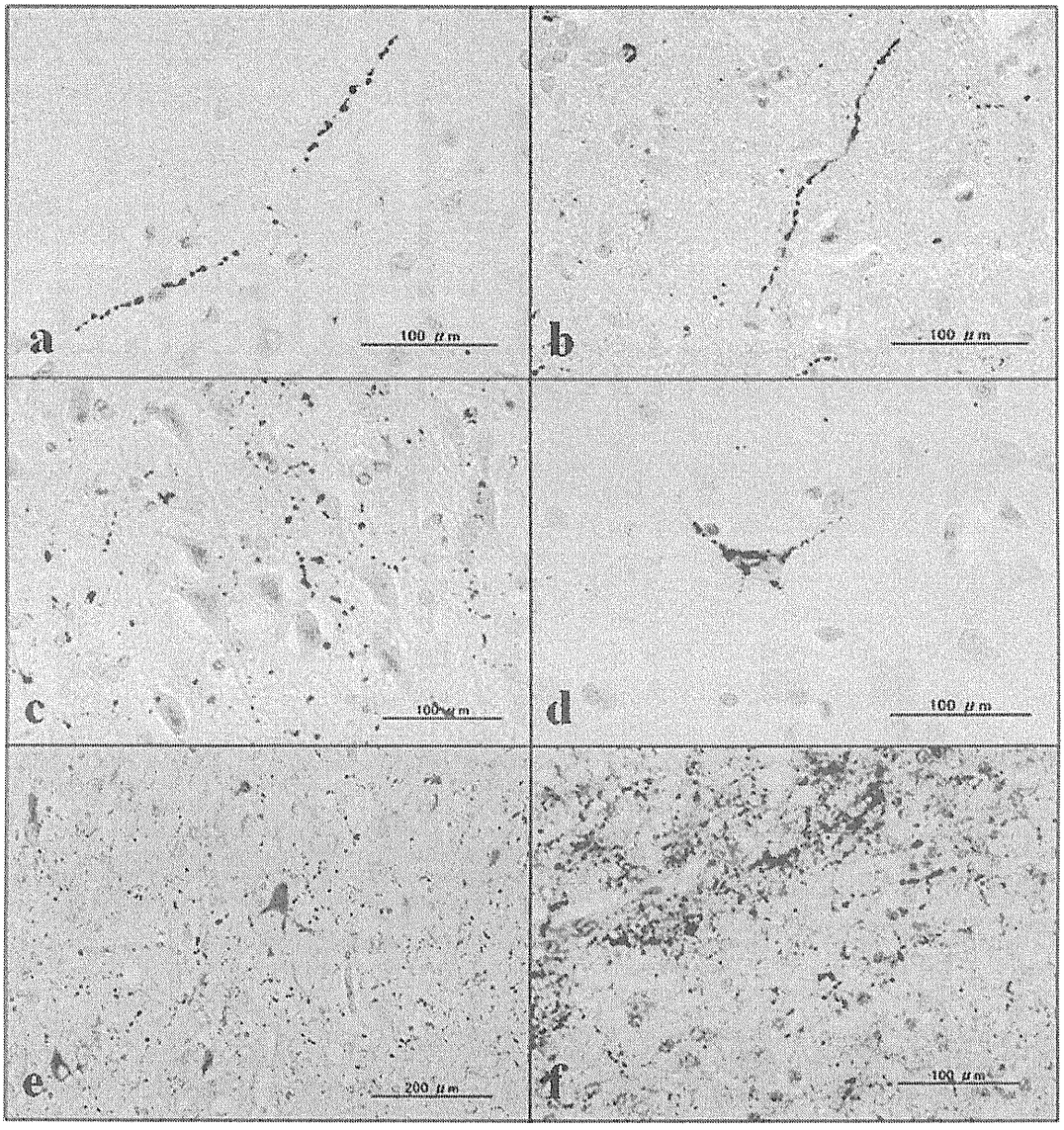

Colour

Figure 3. γ-Secretase activating protein (GSAP) expression in Alzheimer's disease (AD) and control brains. The panels (**a–d**) represent GSAP immunoreactivity of (**a**) beads and string-like deposits in neuronal processes in the frontal cortex of AD, (**b**) beads and string-like deposits in neuronal processes in the frontal cortex of myotonic dystrophy, (**c**) diffuse dot-like deposits in the neuropil and neuronal processes in the hippocampal CA3 region of amyotrophic lateral sclerosis (ALS), (**d**) fine granular deposits in the neuronal cytoplasm in the frontal cortex of normal control, (**e**) double labelling of tau (AT8; red) and GSAP (brown; diffuse dot-like deposits in the neuropil) in the hippocampal CA2 region of ALS, and (**f**) double labelling of tau (AT8; red) and GSAP (brown; diffuse dot-like deposits in the neuropil) in the hippocampal CA3 region of AD.

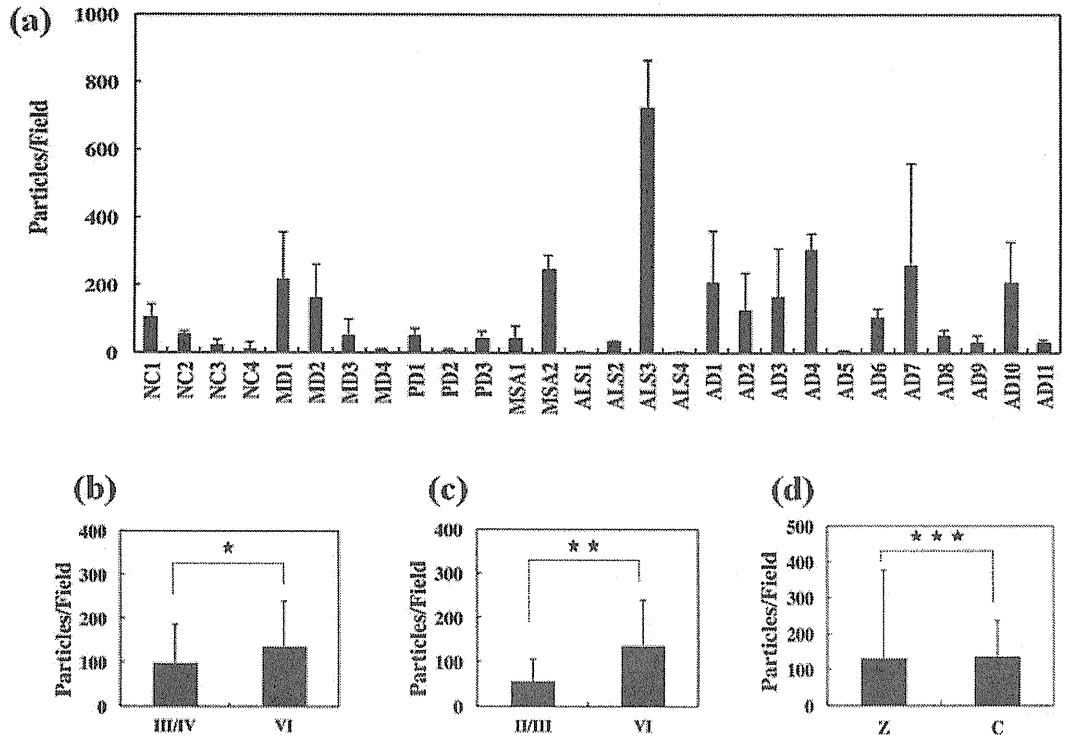

Figure 4. Quantification of γ-secretase activating protein (GSAP)-immunoreactive particles in the hippocampus of Alzheimer's disease (AD) and control brains. The number of diffuse dot-like deposits was counted by imaging of three fields of hippocampal CA2 and CA3 regions with ImageJ software. The panels (**a–c**) represent (**a**) the average of counts/field in individual case expressed as the bar with standard deviation, (**b**) the average of counts/field compared between AD cases categorized into the Braak stage VI ($n = 11$) and non-AD cases categorized into the stages III/IV ($n = 5$), (**c**) the average of counts/field compared between AD cases categorized into the stage VI ($n = 11$) and non-AD cases categorized into the stages II/III ($n = 9$), and (**d**) the average of counts/field compared between the cases with almost no amyloid-β (Aβ) deposits classified as the stage Zero (Z) of amyloid deposition ($n = 8$) and those with extensive Aβ deposits classified as the stage C of amyloid deposition ($n = 13$). The single star (panel **b**) indicates the statistical difference with $P = 0.462$; double stars (panel **c**) indicate the difference with $P = 0.043$; and triple stars (panel **d**) indicate the difference with $P = 0.926$. NC, normal control; MD, myotonic dystrophy; PD, Parkinson's disease; MSA, ••; ALS, amyotrophic lateral sclerosis.

12

towards accumulation of greater amounts of GSAP-immunoreactive particles in the hippocampus of more advanced stages of the disease defined by NFT irrespective of Aβ accumulation.

The close association of GSAP-immunoreactive deposits with PS1 and Aβ in AD brains

Finally, we investigated the association of GSAP-immunoreactive deposits with the potential interacting partner PS1 and the end-product Aβ. PS1 was intensely expressed and ubiquitously distributed in the neuronal cytoplasm and processes, and in addition, less intensely expressed in the neuropil, where GSAP-immunoreactive nodular, patchy and dot-like deposits were often in close contact with PS1 immunoreactivity (arrows in Figure 5**a,b**). Furthermore, GSAP-immunoreactive dense nodular, patchy and dot-like deposits were often located on the core and in the periphery of senile plaques that were labelled with Aβ (Figure 5**c–e**). In contrast, GSAP immunoreactivity was essentially differentiated from AT8-positive tau immunoreactivity (Figure 3**e,f**). The anti-PION non-GSAP antibody HPA023994 reacted with extremely small numbers of granular and nodular deposits (Figure 5**f**), indicating that the great majority of GSAP-immunoreactive deposits labelled with the anti-PION

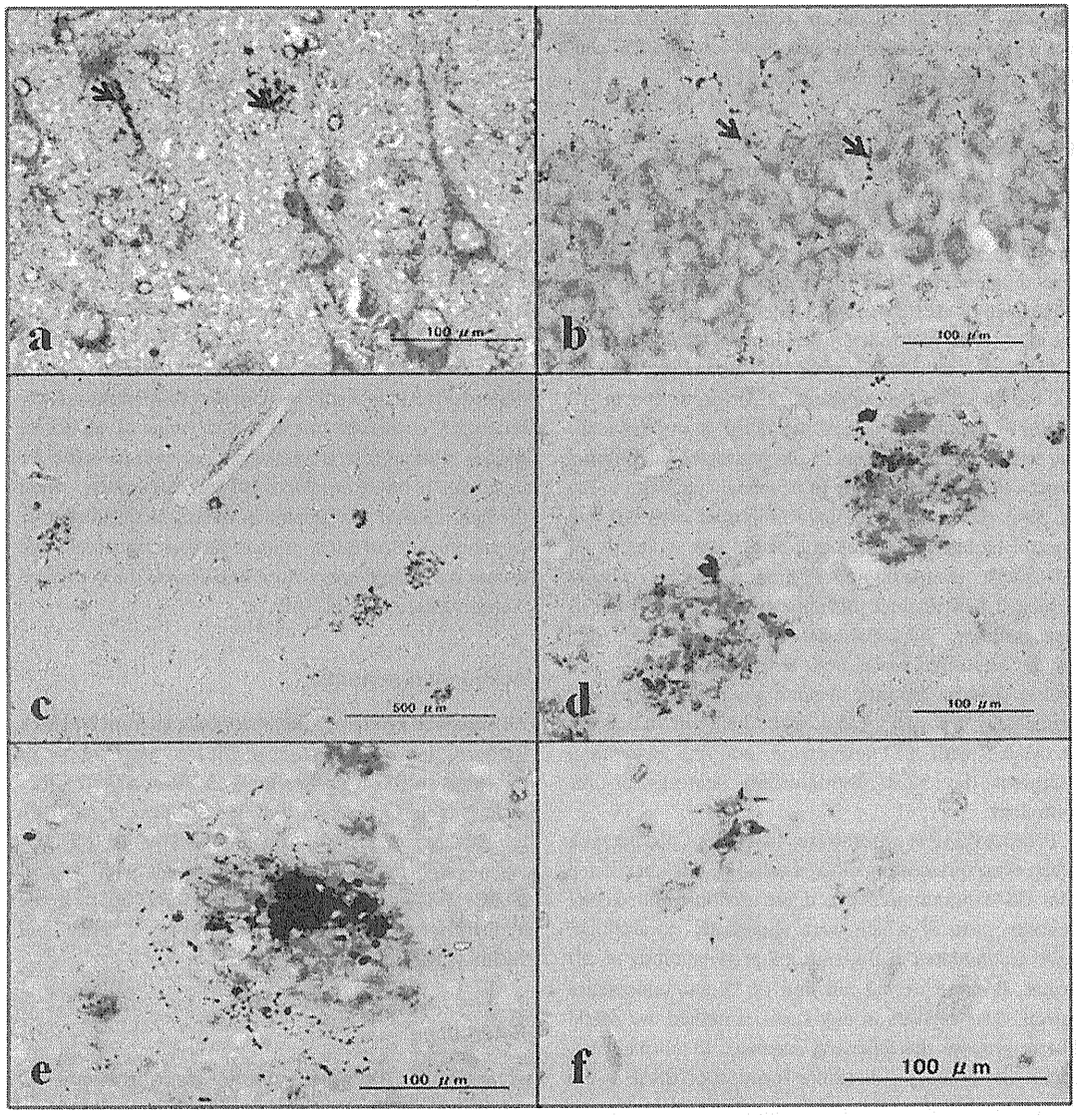

Colour

Figure 5. Close association of γ-secretase activating protein (GSAP) with presenilin-1 (PS1) and amyloid-β (Aβ). The panels (**a–f**) represent (a) double labelling of PS1 (red) and GSAP (brown; dot-like deposits in the neuronal processes and the neuropil) in the frontal cortex of Alzheimer's disease (AD) where the arrows indicate the close contact between GSAP and PS1, (b) double labelling of PS1 (red) and GSAP (brown; dot-like deposits in the neuropil) in the granule cell layer of the hippocampal dentate gyrus of AD where the arrows indicate the close contact between GSAP and PS1, (c) low magnification photograph of double labelling of Aβ (red) and GSAP (brown) in the frontal cortex of AD, (d) high magnification photograph of (c), (e) double labelling of Aβ (red) and GSAP (brown; a clump of dense nodular deposits and many dot-like deposits) in the frontal cortex of AD, and (f) PION immunoreactivity labelled with anti-PION non-GSAP antibody HPA023994 in the frontal cortex of AD.

antibody HPA020058 do not represent the full-length PION protein, but reflect the processed form of PION containing the C-terminal GSAP segment.

Discussion

γ-Secretase activating protein acts as a key molecule responsible for the rate-limiting step in Aβ production by interacting with PS1-CTF and the juxtamembrane region of APP-CTF [5]. Because GSAP modulates γ-cleavage of APP but not of Notch, it would serve as an ideal target molecule for designing γ-secretase modulators with least side effects for AD therapy [6]. Here we for the first time characterized GSAP expression in AD brains by immunohistochemistry. GSAP-immunoreactive deposits are located chiefly in the neuropil and neuronal processes, and occasionally in neuronal cytoplasm in the cerebral cortex and the hippocampus of both AD and control brains, indicating that it did not represent an AD-specific biomarker. GSAP-immunoreactive deposits exhibited four distinct morphological features, such as fine granular cytoplasmic deposits, dense nodular and patchy deposits, beads and string-like deposits, and diffuse dot-like deposits. Among them, dense nodular and patchy deposits, located in the neuropil and closely associated with PS1 expression and Aβ deposition, represent the most distinguishing features of AD pathology.

Because GSAP is concentrated in a trans-Golgi network when overexpressed in cultured cells [5], it is unexpected that GSAP-immunoreactive dense nodular and patchy deposits, most of which were apparently extracellular, were accumulated in the neuropil predominantly of AD brains. Because we did not find GSAP-immunoreactive intranuclear deposits in any cases examined, we would like to propose the following scenario. In normal neurones, the primary subcellular location of GSAP is the
7 cytoplasm, including ER and Golgi, distributed widely in neuronal processes via axonal and dendritic transport. Under physiological conditions, a fine balance between production and turnover of GSAP maintains it at very low constitutive levels, resulting in no obvious accumulation of dense nodular and patchy GSAP deposits. By contrast, in degenerating neurones of AD brains, aberrant regulation of GSAP expression, processing, transport and turnover induces formation of intracellular and extracellular aggregates, which are potentially associated with acceleration of Aβ overproduction.

γ-Secretase activating protein is derived from a C-terminal fragment of PION via an unknown processing mechanism. By bioinformatics analysis, we found that PION exists in the genomes of *Homo sapiens* (Entrez Gene ID 54103), *Pan troglodytes* (472424), *Bos taurus* (615147), *Canis lupus familiaris* (475903), *Mus musculus* (212167), *Rattus norvegiucus* (311984), *Gallus gallus* (417724) and *Danio rerio* (100151358). Importantly, the GSAP fragment corresponding to amino acid residues of 733-854 of the human PION protein is highly conserved through evolution except for the rat. Although the rat PION mRNA sequence (NM_001107845.1) represents a provisional one, it is almost completely devoid of GSAP (Figure S3). These results suggest that GSAP plays an evolutionarily conserved role in a wide range of vertebrate species, although it is unlikely to be indispensable for mammalian brain development and maturation, when the lack of GSAP is validated in the rat. Detailed characterization of GSAP distribution in various animal cells and tissues is seemingly important to elucidate the conserved biological function of GSAP.

Acknowledgements

All autopsied brain samples were obtained from Research Resource Network (RRN), Japan. This work was supported by grants to J-IS from Research on Intractable Diseases (H21-Nanchi-Ippan-201 and H22-Nanchi-Ippan-136), the Ministry of Health, Labour and Welfare (MHLW), Japan, and the High-Tech Research Center Project (S0801043) and the Grant-in-Aid (C22500322), the Ministry of Education, Culture, Sports, Science and Technology (MEXT), Japan.

References

1 Selkoe DJ. Alzheimer's disease: genes, proteins, and therapy. *Physiol Rev* 2001; **81**: 741–66
2 De Strooper B, Annaert W. Novel research horizons for presenilins and γ-secretases in cell biology and disease. *Annu Rev Cell Dev Biol* 2010; **26**: 235–60
3 Wolfe MS. Inhibition and modulation of γ-secretase for Alzheimer's disease. *Neurotherapeutics* 2008; **5**: 391–8
4 Netzer WJ, Dou F, Cai D, Veach D, Jean S, Li Y, Bornmann WG, Clarkson B, Xu H, Greengard P. Gleevec inhibits β-amyloid production but not Notch cleavage. *Proc Natl Acad Sci U S A* 2003; **100**: 12444–9
5 He G, Luo W, Li P, Remmers C, Netzer WJ, Hendrick J, Bettayeb K, Flajolet M, Gorelick F, Wennogle LP, Greengard P. Gamma-secretase activating protein is a

therapeutic target for Alzheimer's disease. *Nature* 2010; **467**: 95–8
6 St George-Hyslop P, Schmitt-Ulms G. Alzheimer's disease: selectively tuning γ-secretase. *Nature* 2010; **467**: 36–7
7 Mirra SS, Gearing M, McKeel DW Jr, Crain BJ, Hughes JP, van Belle G, Heyman A. The Consortium to Establish a Registry for Alzheimer's Disease (CERAD). Part II. Standardization of the neuropathologic assessment of Alzheimer's disease. *Neurology* 1991; **41**: 479–86
8 Misawa T, Arima K, Mizusawa H, Satoh J. Close association of water channel AQP1 with amyloid-β deposition in Alzheimer disease brains. *Acta Neuropathol* 2008; **116**: 247–60
9 Satoh J, Tabunoki H, Arima K. Molecular network analysis suggests aberrant CREB-mediated gene regulation in the Alzheimer disease hippocampus. *Dis Markers* 2009; **27**: 239–52
10 Shioya M, Obayashi S, Tabunoki H, Arima K, Saito Y, Ishida T, Satoh J. Aberrant microRNA expression in the brains of neurodegenerative diseases: miR-29a decreased in Alzheimer disease brains targets neurone navigator 3. *Neuropathol Appl Neurobiol* 2010; **36**: 320–30
11 Braak H, Braak E. Neuropathological stageing of Alzheimer-related changes. *Acta Neuropathol* 1991; **82**: 239–59
12 Braak H, Alafuzoff I, Arzberger T, Kretzschmar H, Del Tredici K. Staging of Alzheimer disease-associated neurofibrillary pathology using paraffin sections and immunocytochemistry. *Acta Neuropathol* 2006; **112**: 389–404

Received 8 February 2011
Accepted after revision 27 June 2011
Published online Article Accepted on 30 June 2011

Supporting information

Additional Supporting Information may be found in the online version of this article:

Figure S1. Western blot of γ-secretase activating protein (GSAP). The present study utilized a rabbit anti-GSAP antibody (HPA020058; Sigma, St. Louis, MO, USA) or a rabbit anti-PION non-GSAP fragment antibody (HPA023994; Sigma). The precise amino acid sequences of the antigens are specified in the *Materials and methods* section. The specificity of the antibodies was validated by Western blot of corresponding recombinant protein fragments tagged with V5 expressed in HEK293 cells. The panels (**a–f**) represent the blots of (a–left, **d**, **e**) HPA020058, (a–right) HPA023994, (**b**) V5, (**c**) heat shock protein 60, an internal control of protein loading, and (**f**) 14-3-3 (K-19), an internal control of protein loading. The lanes (1–12) represent (1, 3, 5) non-transfected cells, (2, 6) the cells transfected with the vector expressing GSAP covering amino acid residues 734-854, (4) the cells transfected with the vector expressing non-GSAP PION covering amino acid residues 427-567, and 80 μg SDS-soluble protein extract isolated from the frontal cortex of (7) NC2, (8) NC3, (9) ALS2, (10) ALS3, (11) AD3 and (12) AD5. IgH indicates non-specific bands corresponding to the immunoglobulin heavy chain. The position of molecular weight marker is indicated on the left.

Figure S2. Preabsorption of anti-γ-secretase activating protein (GSAP) antibody with recombinant GSAP protein. Recombinant GSAP protein covering amino acid residues 734-854 tagged with Xpress was expressed in *E. coli*, purified, gel-separated and blotted. The anti-GSAP antibody (HPA020058) was incubated at 4°C overnight with the recombinant GSAP protein, and then processed for immunohistochemistry. The panels (**a–c**) represent (**a**) Western blot of recombinant GSAP protein by using the antibody HPA020058 (lane 1) and anti-Xpress antibody (lane 2), (**b**) immunohistochemistry of the hippocampal CA3 region of Alzheimer's disease by using the non-absorbed antibody, and (**c**) immunohistochemistry of the same region by using the preabsorbed antibody.

Figure S3. Multiple sequence alignment of γ-secretase activating protein (GSAP) derived from various species. Amino acid sequences of the GSAP segment of PION of various species and pigeon of *Drosophila melanogaster* are aligned by using CLC Free Workbench version 4.5.1 (CLC Bio, Aarhus, Denmark). They are derived from the GenBank data under the accession number of *Homo sapiens* (Entrez Gene ID 54103), *Pan troglodytes* (472424), *Bos taurus* (615147), *Canis lupus familiaris* (475903), *Mus musclus* (212167), *Rattus norvegiucus* (311984), *Gallus gallus* (417724), *Danio rerio* (100151358) and *Drosophila melanogaster* (35200).

Table S1. The cases examined in the present study.

Please note: Wiley-Blackwell are not responsible for the content or functionality of any supporting materials supplied by the authors. Any queries (other than missing material) should be directed to the corresponding author for the article.

NEUROPATHOLOGY

Neuropathology 2011; ••, ••–••

doi:10.1111/j.1440-1789.2011.01256.x

Original Article

Phosphorylated Syk expression is enhanced in Nasu-Hakola disease brains

Jun-ichi Satoh,[1] Hiroko Tabunoki,[1] Tsuyoshi Ishida,[5] Saburo Yagishita,[6] Kenji Jinnai,[7] Naonobu Futamura,[7] Michio Kobayashi,[8] Itaru Toyoshima,[9] Toshiaki Yoshioka,[10] Katsuhiko Enomoto,[10] Nobutaka Arai,[2] Yuko Saito[3] and Kunimasa Arima[4]

[1]Department of Bioinformatics and Molecular Neuropathology, Meiji Pharmaceutical University, [2]Department of Clinical Neuropathology, Tokyo Metropolitan Institute for Neuroscience, Departments of [3]Laboratory Medicine and [4]Psychiatry, National Center Hospital, NCNP, Tokyo, [5]Department of Pathology and Laboratory Medicine, Kohnodai Hospital, National Center for Global Health and Medicine, Chiba, [6]Department of Pathology, Kanagawa Rehabilitation Center, Kanagawa, [7]Department of Neurology, NHO Hyogo-Chuo Hospital, Hyogo, [8]Department of Neurology, Akita National Hospital and Departments of [9]Neurology and Medical Education Center and [10]Molecular Pathology and Tumor Pathology, Akita University School of Medicine, Akita, Japan

Nasu-Hakola disease (NHD) is a rare autosomal recessive disorder, characterized by progressive presenile dementia and formation of multifocal bone cysts, caused by a loss-of-function mutation of DNAX-activation protein 12 (DAP12) or triggering receptor expressed on myeloid cells 2 (TREM2). TREM2 and DAP12 constitute a receptor/adaptor complex on myeloid cells. The post-receptor signals are transmitted via rapid phosphorylation of the immunoreceptor tyrosine-based activating motif (ITAM) of DAP12, mediated by Src protein tyrosine kinases, followed by binding of phosphorylated ITAM to Src homology 2 (SH2) domains of spleen tyrosine kinase (Syk), resulting in autophosphorylation of the activation loop of Syk. To elucidate the molecular mechanism underlying the pathogenesis of NHD, we investigated Syk expression and activation in the frontal cortex and the hippocampus of three NHD and eight control brains by immunohistochemistry. In NHD brains, the majority of neurons expressed intense immunoreactivities for Syk and Y525/Y526-phosphorylated Syk (pSyk) chiefly located in the cytoplasm, while more limited populations of neurons expressed Src. The levels of pSyk expression were elevated significantly in NHD brains compared with control brains. In both NHD and control brains, substantial populations of microglia and macrophages expressed pSyk, while the great majority of reactive astrocytes and myelinating oligodendrocytes did not express pSyk, Syk or Src. These observations indicate that neuronal expression of pSyk was greatly enhanced in the cerebral cortex and the hippocampus of NHD brains, possibly via non-TREM2/DAP12 signaling pathways involved in Syk activation.

Key words: KeyMolnet, Nasu-Hakola disease, phosphorylation, Src, Syk.

INTRODUCTION

Nasu-Hakola disease (NHD; OMIM 221770), also designated polycystic lipomembranous osteodysplasia with sclerosing leukoencephalopathy (PLOSL), is a rare autosomal recessive disorder, characterized by progressive presenile dementia and formation of multifocal bone cysts.[1,2] Typically, patients show pathological bone fractures during the third decade of life, and a frontal lobe syndrome such as loss of social inhibitions during the fourth decade of life, followed by profound dementia and loss of mobility.[3] The neuropathological hallmark of NHD includes extensive demyelination, accumulation of axonal spheroids, and intense astrogliosis predominantly in the frontal and temporal lobes and the basal ganglia.[4]

NHD is caused by a homozygous mutation located in one of the two genes, DNAX-activation protein 12 (DAP12), alternatively named TYRO protein tyrosine kinase-binding protein (TYROBP) on chromosome 19q13.1 or triggering receptor expressed on myeloid cells 2 (TREM2) on chromosome 6p21.1. Currently, 17 different

Correspondence: Jun-ichi Satoh, MD, Department of Bioinformatics and Molecular Neuropathology, Meiji Pharmaceutical University, 2-522-1 Noshio, Kiyose, Tokyo 204-8588, Japan. Email: satoj@my-pharm.ac.jp

Received 24 June 2011; revised and accepted 22 August 2011.

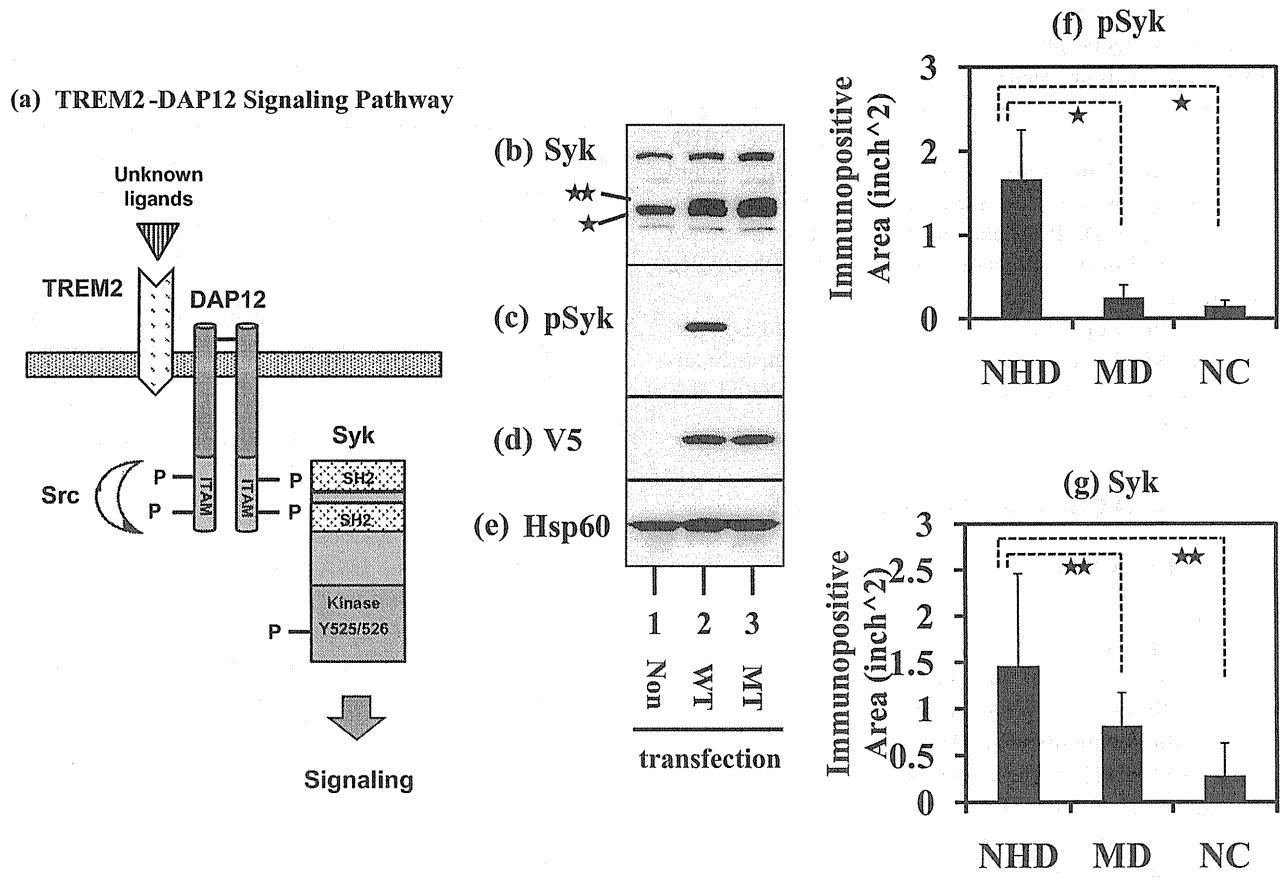

Fig. 1 Triggering receptor expressed on myeloid cells 2 (TREM2) – DNAX-activation protein 12 (DAP12) signaling pathway, validation of anti-pSyk (anti-phosphorylated spleen tyrosine kinase) antibody, and morphometric data.
(a) TREM2-DAP12 signaling pathway. TREM2 monomer and DAP12 homodimer constitute a receptor/adaptor complex on myeloid cells. The post-receptor signals are transmitted via rapid phosphorylation of immunoreceptor tyrosine-based activating motif (ITAM) of DAP12 mediated by Src protein tyrosine kinases, followed by binding of phosphorylated ITAM to tandem SH2 domains of Syk, resulting in autophosphorylation of the activation loop of Syk. (b–e) Western blot. The panels (b–e) represent Western blot with antibodies against (b) Syk (a single star indicates a 72-kDa endogenous form, while double stars indicate a 76-kDa exogenous form tagged with V5) (c) Y525/Y526-phosphorylated Syk (d) V5, and (e) heat shock protein Hsp60, an internal control of protein loading. The lanes (1–3) indicate the protein extract of HEK293 cells (1) without transfection and with transfection of expression vectors of (2) the wild-type (Y525/Y526) Syk and (3) the mutant (N525/N526) Syk. (f,g) Immunopositive area. Five images of layer III of the frontal cortex were captured and processed for quantification by ImageJ. The panels (f, g) represent the positive area of (f) pSyk and (g) Syk. A single star indicates $P < 0.01$, while double stars indicate $P > 0.05$ by one-way ANOVA with *post hoc* Turkey's test.

loss-of-function mutations are identified in either DAP12 or TREM2, all of which cause an identical disease phenotype.[5,6]

The trimolecular complex composed of TREM2 monomer and DAP12 homodimer constitutes a receptor/adaptor complex expressed on osteoclasts, dendritic cells, monocytes/macrophages and microglia (Fig. 1, panel a).[7] This complex transmits signals via the immunoreceptor tyrosine-based activating motif (ITAM) of DAP12.[8] Following receptor engagement, ITAM is rapidly phosphorylated on two tyrosine residues by Src protein tyrosine kinases (PTKs). Phosphorylated ITAM provides a docking site for the Src homology 2 (SH2) domains of spleen tyrosine kinase (Syk). Activation of Syk recruited to ITAM promptly transduces downstream signals, including activation of phosphatidylinositol-3 kinase (PI3K), phospholipase C (PLC), protein kinase C (PKC), and mitogen-activated protein kinase (MAPK).[9,10]

The molecular mechanism underlying development of leukoencephalopathy in NHD remains largely unknown. DAP12-deficient mice develop osteopetrosis, hypomyelinosis and synaptic degeneration, suggesting that DAP12 signaling is pivotal for development of osteoclasts and oligodendrocytes, and synaptogenesis in mice.[11,12] Furthermore, the number of microglia is greatly reduced in the brain of DAP12-deficient/loss-of-function

mice.[13,14] Crosslinking of TREM2 on cultured mouse microglia triggers phagocytosis of apoptotic neurons.[15] These observations suggest that loss of essential biological functions of DAP12/TREM2-deficient microglia plays a central role in the pathogenesis of NHD. However, by immunohistochemistry, we recently found that TREM2 is not expressed constitutively on human microglia, and DAP12-deficient Iba1-positive microglia are preserved in the brains of NHD patients with DAP12 mutations.[16]

To extend our previous study, we characterized Syk activation in NHD and control brains by immunohistochemistry, and unexpectedly found that phosphorylated Syk expression is greatly enhanced in NHD brains.

MATERIALS AND METHODS

Human brain tissues

The brain tissues were obtained from Research Resource Network (RRN), Japan. Written informed consent was taken in all the cases at autopsy, following the regulation of the institutional ethics committees. The present study includes three patients with NHD, composed of a 42-year-old man (NHD1), a 48-year-old woman (NHD2) and a 44-year-old man (NHD3), four neurological disease controls affected with myotonic dystrophy (MD), composed of a 68-year-old man (MD1), a 61-year-old man (MD2), a 60-year-old man (MD3) and a 53-year-old woman (MD4), and four subjects who died of non-neurological causes (NC), composed of a 63-year-old man who died of prostate cancer and acute myocardial infarction (NC1), a 67-year-old man who died of dissecting aortic aneurysm (NC2), a 57-year-old man who died of alcoholic liver cirrhosis (NC3) and a 61-year-old man who died of rheumatoid arthritis with interstitial pneumonia (NC4). We selected MD patients for neurological disease controls because they are associated with early-onset global intellectual impairment. To compare the results with those of the most advanced demented cases, we additionally included four patients with Alzheimer's disease (AD), composed of a 59-year-old man (AD1), a 68-year-old woman (AD2), a 72-year-old man (AD3) and a 77-year-old woman (AD4). All AD cases were categorized into stage C of amyloid deposition and stage VI of neurofibrillary degeneration following the Braak staging system. The regions examined include the frontal cortex, the hippocampus and the basal ganglia in NHD cases, and the frontal cortex and the hippocampus in MD, NC and AD cases. The homozygous mutation of a single base deletion of 141G (141delG) in exon 3 of DAP12 was identified in NHD1 and NHD2, while the genetic analysis was not performed in NHD3.[16]

Immunohistochemistry

After deparaffination, tissue sections were heated in 10 mmol citrate sodium buffer by autoclaving them in a temperature-controlled pressure chamber (Dako, Tokyo, Japan). They were exposed to 3% hydrogen peroxide-containing methanol at room temperature (RT) for 15 min to block the endogenous peroxidase activity. The tissue sections were then incubated with phosphate-buffered saline (PBS) containing 10% normal goat serum at RT for 15 min to block non-specific staining. They were incubated in a moist chamber at 4°C overnight with rabbit anti-Syk antibody (sc-1077; Santa Cruz Biotechnology, Santa Cruz, CA, USA) at a dilution of 1:2000 of 200 μg/mL stock solution, rabbit anti-phosphorylated Syk (pSyk) antibody (AP3271a; ABGENT, San Diego, CA, USA) at a dilution of 1:200 of 250 μg/mL stock solution, or rabbit anti-Src antibody (11097-1-AP; ProteinTech Group, Chicago, IL, USA) at a dilution of 1:220 of 200 μg/mL stock solution. The antibody sc-1077 was generated against an N-terminal peptide of the human Syk protein, while the antibody AP3271a was raised against a synthetic phosphopeptide corresponding to amino acid residues surrounding Y525/Y526 located in the activation loop of human Syk.[17] Therefore, the antibody AP3271a reacts strictly with an activated form of the Syk protein *in situ*. After washing with PBS, the tissue sections were labeled at RT for 30 min with a horseradish peroxidase (HRP)-conjugated secondary antibody (Nichirei, Tokyo, Japan), followed by incubation with a colorizing solution containing diaminobenzidine tetrahydrochloride (DAB). All the sections were exposed to a counterstain with hematoxylin. For negative controls, the step of incubation with primary antibodies was omitted.

To identify the cell types, the serial sections were stained with antibodies against GFAP (N1560; Dako) for astrocytes, Iba1 (019-19741; Wako Pure Cehmical, Osaka, Japan), CD68 (N1577; Dako), and DAP12 (sc-20783; Santa Cruz Biotechnology) for macrophages/microglia, and myelin basic protein (MBP) (N1564; Dako) for myelin/myelinating oligodendrocytes, as previously described.[16]

Quantification of immunoreactivity

To quantify pSyk and Syk immunoreactivities, the images derived from five fields of layer III of the frontal cortex at 200 × magnification were captured on an Olympus BX51 universal microscope, and they were processed for quantification by using ImageJ software (National Institute of Health, Bethesda, MD, USA). The difference in the average of immunopositive areas between NHD and controls was evaluated statistically by one-way analysis of variance (ANOVA) followed by *post hoc* Turkey's test.

Western blot analysis

The full-length human Syk sequence was amplified by PCR, and cloned into the expression vector pEF6/V5-His TOPO (Invitrogen, Carlsbad, CA, USA). Two consecutive amino acid residues Y525/Y526 were converted to N525/N526 by using QuikChange II XL site-directed mutagenesis kit (Stratagene, La Jolla, CA, USA), and they were validated by direct sequencing analysis. The vector containing either the wild-type or the mutated sequence was transfected in HEK293 cells by using Lipofectamine 2000 reagent (Invitrogen).

To prepare total protein extract, the cells were homogenized in RIPA buffer supplemented with a cocktail of protease inhibitors and tyrosine protein phosphatase inhibitors (Sigma, St. Louis, MO, USA). The protein extract was centrifuged at 13 400 × *g* for 5 min at RT, separated on a 12% SDS-PAGE gel, and transferred onto nitrocellulose membranes. They were repeatedly immunolabeled at RT overnight with rabbit anti-pSyk antibody (AP3271a), rabbit anti-Syk antibody (sc-1077), mouse anti-V5 antibody (Invitrogen), or goat anti-heat shock protein HSP60 antibody (sc-1052, N-20; Santa Cruz Biotechnology) used for an internal control of protein loading. Then, the membranes were incubated at RT for 60 min with HRP-conjugated anti-rabbit, anti-mouse, or anti-goat IgG (Santa Cruz Biotechnology). The specific reaction was visualized by exposing the membranes to a chemiluminescent substrate (Thermo Scientific, Rockford, IL, USA).

RESULTS

Validation of the specificity of anti-phosphorylated Syk antibody by Western blot

First, we validated the specificity of anti-pSyk antibody AP3271a by Western blot of protein extract of HEK293 cells after introduction of exogenous Syk transgenes. Both the wild-type human Syk protein (Y525/Y526) and the mutant form (N525/N526), tagged with V5, were expressed transiently in HEK293 cells. The anti-Syk antibody sc-1077 reacted with a 72-kDa endogenous form, along with a 76-kDa V5-tagged exogenous form (Fig. 1, panel b, lanes 1–3). Importantly, the anti-pSyk antibody AP3271a reacted specifically with the exogenous Syk autophosphorylated on Y525/Y526, but did not react with the nonphosphorylatable counterpart having N525/N526 instead of Y525/Y526 (Fig. 1, panel c, lanes 1–3).

Neuronal phosphorylated Syk expression was enhanced in NHD brains

Next, we studied Syk, pSyk, and Src expression in the brains of three NHD patients, four myotonic dystrophy (MD) patients, and four non-neurological (NC) subjects by immunohistochemistry. In the frontal cortex and the hippocampus of NHD brains, the majority of neurons expressed intense/intermediate immunoreactivities for pSyk and Syk chiefly located in the cytoplasm (Fig. 2, panels a, b; Fig. 3, panels a, b, e). More limited populations of neurons expressed intense/intermediate immunoreactivity for Src in both NHD1 and NHD2 brains (Fig. 3, panel f), while a very small population of neurons expressed Src in the NHD3 brain. The antibody against Syk or Src, to some extent, stained the neuropil in NHD brains (Fig. 3, panels e, f). Great numbers of GFAP-positive astrocytes and Iba1-positive microglia were accumulated chiefly in the white matter and to a lesser extent in the gray matter of the cerebral cortex, the hippocampus and the basal ganglia of NHD brains, where DAP12 immunoreactivity was completely absent in microglia (not shown).

Although pSyk immunoreactivity was detected in the cytoplasm of neurons in the cerebral cortex and the hippocampus of NC and MD brains (Fig. 2, panels d–f), quantitative analysis indicated that the pSyk-immunopositive area was significantly greater in NHD brains, compared with the area in control brains ($P < 0.01$ by one-way ANOVA with *post hoc* Turkey's test) (Fig. 1, panel f). Furthermore, a subpopulation of neurons in NHD brains expressed intense pSyk immunoreactivity in the nuclei in addition to the cytoplasm (Fig. 2, panel a inset). These observations indicated that neuronal pSyk expression is greatly enhanced in NHD brains.

In both NHD and control brains, substantial populations of microglia and macrophages expressed cytoplasmic pSyk immunoreactivity at varying intensities (Fig. 3, panels a,c). In contrast, the vast majority of surviving oligodendrocytes and reactive astrocytes, existing in the demyelinating white matter of NHD brains, did not express Syk, pSyk, or Src. In addition, both myelinating oligodendrocytes and reactive astrocytes in control brains did not exhibit Syk, pSyk or Src.

Syk expression levels showed a trend for enhancement in NHD brains, compared with the levels in control brains. However, the differences did not reach a statistical significance ($P > 0.05$ by one-way ANOVA with *post hoc* Turkey's test) (Fig. 1, panel g). pSyk and Src but not Syk were concentrated in cytoplasmic granules of hippocampal neurons, most evident in those located in the subiculum presenting with characteristics of granulovacuolar degeneration (GVD), which were found only in MD and NC cases (Fig. 3, panel d and d inset).

Neuronal expression of phosphorylated Syk was found in AD brains

Finally, we studied pSyk expression in the brains of four AD patients by immunohistochemistry. In the frontal

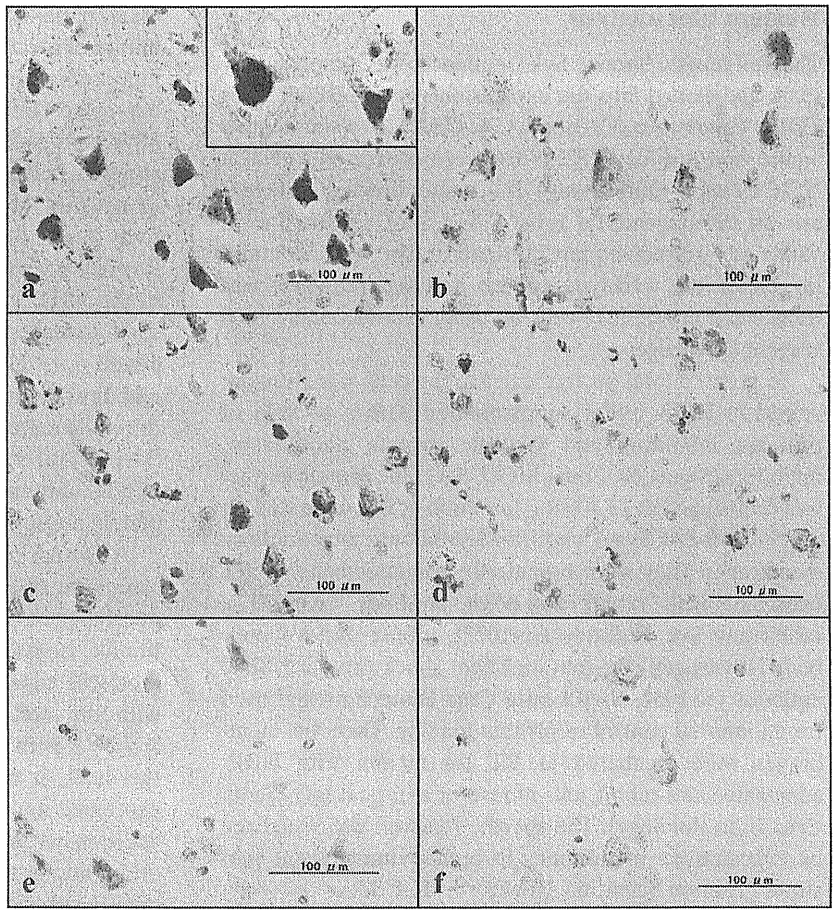

Fig. 2 pSyk (phosphorylated spleen tyrosine kinase) expression in Nasu-Hakola disease (NHD) and control brains. Formalin-fixed paraffin-embedded tissue sections of three NHD, four myotonic dystrophy (MD), and four non-neurological control (NC) brains were processed for immunohistochemistry. The panels (a–f) represent the frontal cortex of (a) NHD1, pSyk (inset: nuclear and cytoplasmic expression) (b) NHD2, pSyk (c) NHD3, pSyk (d) MD1, pSyk (e) NC3, pSyk, and (f) NC4, pSyk.

cortex of AD brains, neurons and microglia expressed pSyk immunoreactivity in the cytoplasm (Fig. 4, panels a, b). However, the number of pSyk-immunoreactive neurons and the intensity of pSyk immunoreactivity varied among the four cases. In contrast, almost all hippocampal pyramidal neurons expressed intense pSyk immunoreactivity in all AD brains (Fig. 4, panel c). Furthermore, GVD granules were always labeled with the anti-pSyk antibody (Fig. 4, panel d). These results suggest that enhanced expression of pSyk in neurons does not represent an NHD-specific phenomenon but may reflect a not yet defined neurodegenerative process.

DISCUSSION

Nasu-Hakola disease is caused by a loss-of-function mutation of DAP12 or TREM2. TREM2 and DAP12 constitute a receptor/adaptor complex on myeloid cells, including osteoclasts and dendritic cells. At present, the precise TREM2 ligands *in vivo* remain uncharacterized (Fig. 1, panel a). DAP12 also associates with several immunoreceptors other than TREM2, such as triggering receptor expressed on myeloid cells 1 (TREM1), signal-regulatory protein beta 1 (SIRPB1), and myeloid DAP12-associating lectin 1 (MDL1).[8] The post-receptor signals are transmitted via rapid phosphorylation of ITAM of DAP12, mediated by Src family PTKs, followed by binding of phosphorylated ITAM to two tandem SH2 domains of Syk, resulting in autophosphorylation of the activation loop of Syk.[9,10,17] Recently, we found that TREM2 is not expressed constitutively on microglia, and DAP12-deficient Iba1-positive microglia are well preserved in the brains of NHD patients with DAP12 mutations.[16] In the present study, we showed that neuronal expression of pSyk, an activated form of Syk, is greatly enhanced in the cerebral cortex and the hippocampus of NHD brains compared with the levels of expression in control brains.

Syk is a non-receptor tyrosine kinase expressed on virtually all hematopoietic cells, and plays a key role in the TREM2/DAP12-signaling pathway.[9,10] DAP12 and Fc receptor γ-chain (FcRγ) coordinately regulate development of osteoclasts by transmitting signals via the ITAM-Src-Syk cascade.[18,19] Syk-deficient osteoclast progenitor cells are defective in osteoclastogenesis.[18] Syk regulates

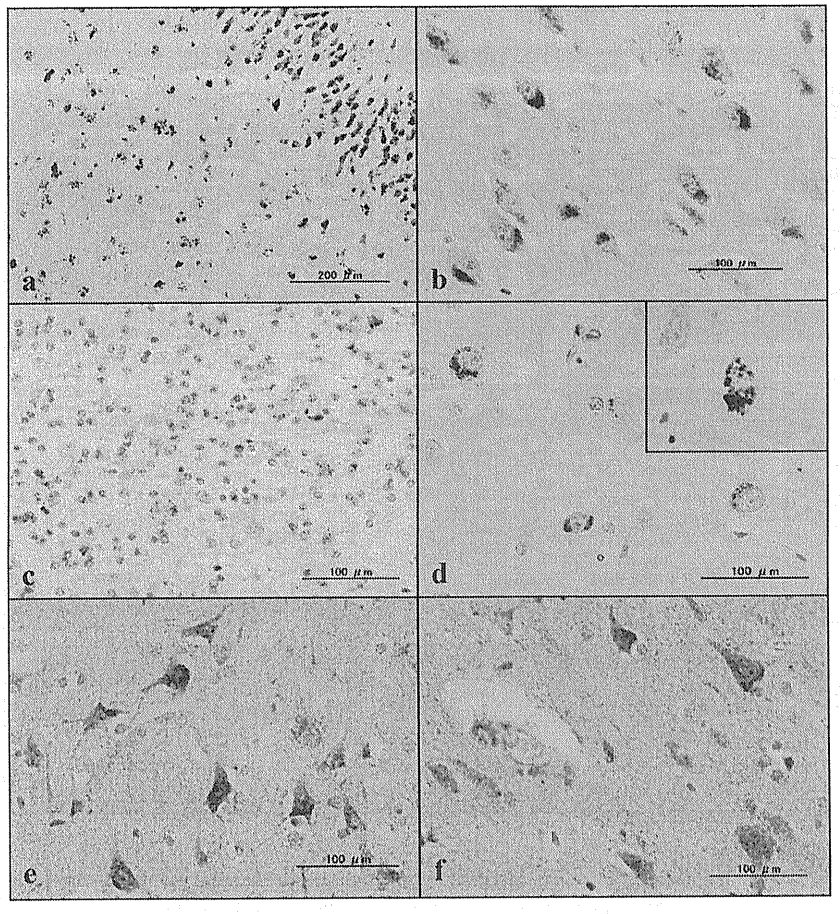

Fig. 3 pSyk (phosphorylated spleen tyrosine kinase), Syk, and Src expression in Nasu-Hakola disease (NHD) and control brains.
The panels (a–f) represent (a) the hippocampus, NHD1, pSyk (b) the hippocampus, NHD2, pSyk (c) the frontal white matter, NHD3, pSyk (d) the subiculum, myotonic dystrophy (MD)4, pSyk (inset: Src) (e) the frontal cortex, NHD2, Syk, and (f) the frontal cortex, NHD2, Src.

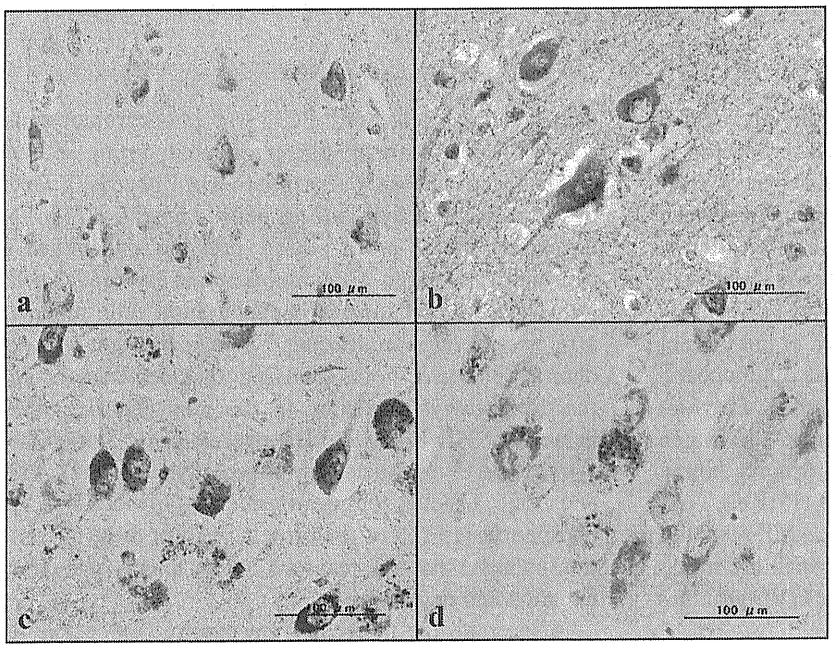

Fig. 4 pSyk (phosphorylated spleen tyrosine kinase) expression in Alzheimer's disease (AD) brains.
Formalin-fixed paraffin-embedded tissue sections of four AD brains were processed for immunohistochemistry. The panels (a–d) represent (a) the frontal cortex, AD1, pSyk (b) the frontal cortex, AD4, pSyk (c) the hippocampus, AD4, pSyk, and (d) the hippocampus, AD1, pSyk.

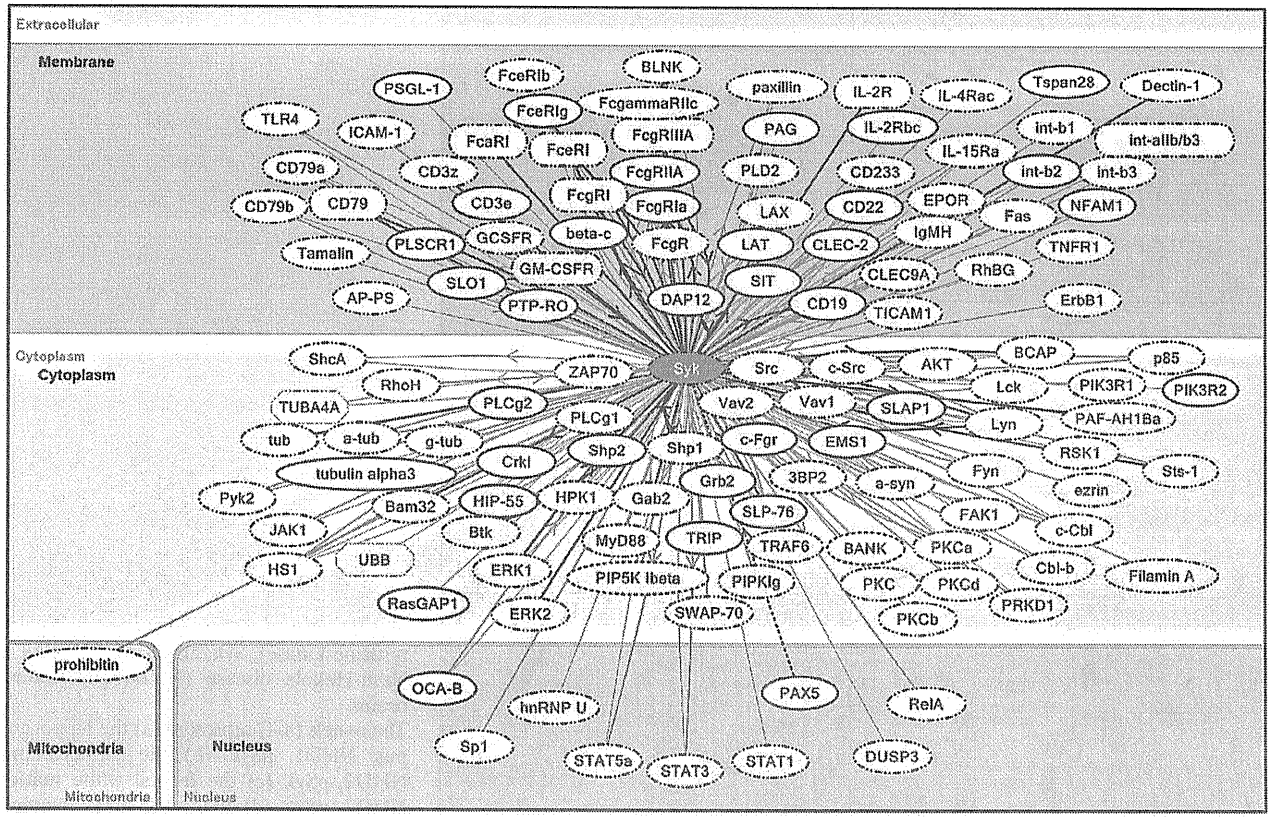

Fig. 5 Molecular network of spleen tyrosine kinase (Syk).
By bioinformatics analysis using KeyMolnet, a tool for analyzing molecular interactions on the comprehensive knowledgebase, the neighboring search within one path from Syk (red node) as a starting point generates the complex molecular network composed of 138 molecules connecting to Syk. They are arranged according to the predicted subcellular location. The connections of thick lines represent the core contents, while thin lines indicate the secondary contents of KeyMolnet. The molecular relation is indicated by solid line without arrow (direct interaction or complex formation), solid line with arrow (direct activation), or dashed line with arrow (transcriptional activation).

chemotaxis of macrophages toward fractalkine by activating PI3K, Rac1 and Cdc42 pathways.[20] Syk is located in both cytoplasmic and nuclear compartments in B cells, where it is exported from the nucleus following prolonged engagement of the B-cell receptor (BCR) and activation of protein kinase C.[21] Interestingly, we identified intense pSyk and Src immunoreactivities, concentrated in GVD granules of hippocampal neurons in MD and NC brains but not in NHD brains. Furthermore, GVD granules of hippocampal neurons in AD brains also expressed pSyk. Previous studies indicate that the active forms of caspase-3, glycogen synthase kinase-3β (GSK-3β), c-Jun N-terminal kinase (JNK), c-Jun, pancreatic eIF2-alpha kinase (PERK), TAR DNA-binding protein-43 (TDP-43), and cAMP-response element-binding protein (CREB), all of which are modified by phosphorylation, are accumulated in GVD granules of hippocampal neurons in AD brains.[22]

Syk expression is also identified in non-hematopoietic cells, such as hepatocytes, fibroblasts, P19 mouse embryonal carcinoma cells and PC12 rat pheochromocytoma cells.[23,24] Syk is tyrosine-phosphorylated during retinoic acid-induced neuronal differentiation of P19 cells, in which overexpression of Syk induces neurite extension.[24] In the developing mouse brain, pSyk expression is identified in neuronal progenitor cells, hippocampal pyramidal cells, retinal ganglion cells and cerebellar granule cells, but not in astrocytes or oligodendrocytes,[25] being consistent with our observations that both surviving oligodendrocytes and reactive astrocytes existing in the demyelinating white matter of NHD brains did not express pSyk. Syk inhibits aggregation of α-synuclein by phosphorylating Y122, Y133 and Y136 residues on α-synuclein.[26] Furthermore, Syk phosphorylates Y18 of tau protein.[27] All of these observations indicate that Syk plays a key role in neuronal differentiation and degeneration.

At present, the molecular mechanism responsible for enhanced neuronal expression of pSyk in NHD brains remains unclear, because TREM2/DAP12 signaling is lost